

Excited D and D_s meson spectroscopy from lattice QCD

Graham Moir*, Michael Peardon, Sinéad M. Ryan, Christopher E. Thomas

School of Mathematics, Trinity College, Dublin 2, Ireland

E-mail: moirg@tcd.ie

(For the Hadron Spectrum Collaboration)

We present highly excited spectra of charm-light and charm-strange mesons from dynamical lattice QCD. Our calculations are performed on anisotropic $N_f = 2 + 1$ dynamical ensembles generated by the Hadron Spectrum Collaboration. The use of novel techniques and a large basis of interpolating operators have allowed us to extract these spectra to a high degree of statistical precision, extract states of high spin and observe candidate hybrid mesons. We interpret and discuss our results in light of the current experimental situation.

Xth Quark Confinement and the Hadron Spectrum

8-12 October 2012

TUM Campus Garching, Munich, Germany

*Speaker.

1. Introduction

The observation of the enigmatic $D_{s0}^*(2317)^\pm$ and $D_{s1}(2460)^\pm$ states at BABAR [1] and CLEO [2] along with the discovery of many unexpected states in the hidden-charm sector, has forced charm physics back into the theoretical and experimental spotlight. The nature of these states is unknown since they do not fit well with current theoretical understanding, i.e. they do not match, or in some cases fit into, the pattern expected by quark potential models [3, 4]. Some of the states have been suggested to be molecular mesons, hybrid mesons (in which the gluonic field is excited) or tetraquarks but the emergence of a common consensus on the nature of any of these states seems unlikely without further work from both experimentalists and theorists.

On the experimental side, BESIII along with the planned PANDA experiment at GSI/FAIR will explore the charm sector in detail, while on the theoretical side, lattice field theory, due to its ab initio nature, is perfectly placed to comment on these unexplained states. For example, we have recently studied the charmonium sector via the extraction of a highly excited spectrum. The results of this study are presented in Refs. [5, 6]. In this proceeding we focus on the open-charm sector, and present highly excited spectrum in both the charm-light and charm-strange cases.

The rest of this paper is organised as follows: in section 2 we give our computational details along with a brief discussion of our operator construction, while also explaining the details of our analysis and spin identification scheme. In section 3 we present the charm-light and charm-strange spectra, interpret our results and compare with experiment.

2. Lattice calculation and analysis

The calculations presented here make use of the anisotropic ensembles generated by the Hadron Spectrum Collaboration [7, 8], in which there are two degenerate dynamical light quarks and a dynamical strange quark ($N_f = 2 + 1$). We use a discretisation in which the spatial lattice spacing, a_s , and the temporal lattice spacing, a_t , are related via $\xi = a_s/a_t \sim 3.5$. This ensures that we simulate with $a_t m_c \ll 1$ and that the standard relativistic formulation of fermions can be used.

The gauge sector is described by a Symanzik-improved anisotropic action with tree-level tadpole improved coefficients while the fermionic fields are described by a tree-level tadpole improved Sheikholeslami-Wohlert anisotropic action with stout-smear spatial links [7, 8]. The same action is used for the charm quark as for the light and strange quarks except that the parameter describing the weighting of spatial and temporal derivatives in the lattice action is chosen to give a relativistic dispersion relation for the η_c meson as described in Ref. [5].

We set the scale by considering the ratio of the Ω -baryon mass measured on these ensembles to the experimental mass. This corresponds to a spatial lattice spacing of $a_s \sim 0.12$ fm and a temporal

Volume	m_π/MeV	N_{cfgs}	N_{tsrcs}	N_{vecs}
$24^3 \times 128$	391	553	16	162

Table 1: The gauge-field ensembles used in this work. N_{cfgs} and N_{tsrcs} are respectively the number of gauge-field configurations and time-sources per configuration used; N_{vecs} refers to the number of eigenvectors used in the distillation method [9].

lattice spacing approximately 3.5 times smaller $a_t^{-1} \sim 5.7$ GeV. Table 1 summarises the ensembles used in our calculation with full details given in Refs. [7, 8].

2.1 Operator construction and spectroscopy on the lattice

In lattice calculations, spectral information is obtained via Euclidean two-point correlation functions,

$$C_{ij}(t) = \langle 0 | \mathcal{O}_i(t) \mathcal{O}_j^\dagger(0) | 0 \rangle, \quad (2.1)$$

where $\mathcal{O}^\dagger(0)$ and $\mathcal{O}(t)$ are the source and sink interpolating fields respectively. When inserting a complete set of eigenstates of the Hamiltonian, the correlation function becomes a spectral decomposition,

$$C_{ij}(t) = \sum_{\mathbf{n}} \frac{Z_i^{\mathbf{n}*} Z_j^{\mathbf{n}}}{2E_{\mathbf{n}}} e^{-E_{\mathbf{n}} t}, \quad (2.2)$$

where the sum is over a discrete set of states due to the finite volume of the lattice. The vacuum-state matrix elements $Z_i^{\mathbf{n}} \equiv \langle \mathbf{n} | \mathcal{O}_i^\dagger | 0 \rangle$, are known as *overlaps* and allow for a spin identification of states as described in section 2.2.

In order to maximise the spectral information we can obtain from correlation functions we use a large basis of operators. We employ the same derivative based operator construction scheme as in Ref. [10] including operators that contain up to three derivatives. We apply the *distillation* [9] smearing procedure to the quark fields in each operator. This provides an efficient method to calculate correlation functions with large bases of operators while also reducing the contamination of noisy UV modes that do not make a significant contribution to the low-energy physics we wish to extract.

The lattice breaks three-dimensional rotational symmetry down to that of the cubic group, O_h . So instead of an infinite number of labels on states, $J \geq 0$, one instead has a finite number of lattice irreps; the five single-cover irreps for states at rest are A_1 , A_2 , E , T_1 and T_2 . States of $J \geq 2$ have their components split across many lattice irreps. For each lattice irrep, Λ^P (where P is parity), and flavour sector (D and D_s), we compute an $N \times N$ matrix of correlation functions (equation 2.1). Here, N is the number of operators used within each lattice irrep as shown in Table 2.

The extraction of spectroscopic states from these *correlation matrices* will be the subject of the next section.

Λ	Λ^-	Λ^+
A_1	18	18
A_2	10	10
T_1	44	44
T_2	36	36
E	26	26

Table 2: The number of operators used in each lattice irrep Λ^P .

2.2 Analysis

We apply the variational method [11, 12] to our correlation matrices in order to find the optimal extraction, in the variational sense, of energies in a given channel. This amounts to solving the generalised eigenvalue problem,

$$C_{ij}(t)v_j^n = \lambda^n(t, t_0)C_{ij}(t_0)v_j^n, \quad (2.3)$$

where an appropriate reference time-slice, t_0 , must be chosen as described in Ref. [10]. The energies are determined by fitting the dependence of the eigenvalues (*principal correlators*), λ^n , on $(t - t_0)$. The eigenvectors v^n are related to the operator-state overlaps, Z , and hence play a vital role in the spin identification of states which is not as straight forward as one might expect.

In principle, the spin of a single-hadron state can be determined by extracting the spectrum at various lattice spacings and then extrapolating to the continuum limit. There, where full rotational symmetry is restored, energy degeneracies between different lattice irreps should emerge. However, there are difficulties with this procedure. First, this requires high precision calculations with successively finer lattice spacings and so with increasing computation cost; this is not practical with currently available resources. Second, the continuum spectrum can exhibit physical near degeneracies and the question arises as to how to identify, without infinite statistics, which degeneracies are due to the lattice discretisation and which are physical degeneracies.

To circumvent these problems we use the spin identification scheme described in Refs. [10, 13] which can be used at a single finite lattice spacing. Lattice operators respect the symmetry of the lattice but they also carry a ‘memory’ of the continuum spin, J , from which they came. If our lattice is reasonably close to restoring continuum symmetry, at least on the hadronic scale, then we expect that an operator coming from a continuum spin J will overlap predominantly onto states of continuum spin J [14]. This has been shown to be the case on these ensembles in many previous studies, for example Ref. [5]. We hence use the operator-state overlaps to perform a spin identification of each extracted state in a given irrep, and use the pattern of the Z values to recombine components of $J \geq 2$ states since components of the same J state spread across different irreps have the same Z values up to discretisation effects. In order to quote masses for the $J \geq 2$ states we perform joint fits to the principal correlators in each irrep as described in Ref. [13].

3. Results

The spin-identified charm-light and charm-strange spectra are shown in Figs. 1 and 2 respectively. The calculated (experimental) masses have had half of the calculated (experimental) η_c mass subtracted from them in order to reduce the systematic error from the tuning of the bare charm quark mass, which is described in Ref. [5]. In Fig. 1, we show the lowest non-interacting $D\pi$ and $D_s\bar{K}$ thresholds from both our calculated values (coarse green dashed) and using experimental values (fine black dashed). The lines in Fig. 2 represent the lowest non-interacting DK threshold, again using our calculated values (coarse green dashed) and experimental values (fine black dashed).

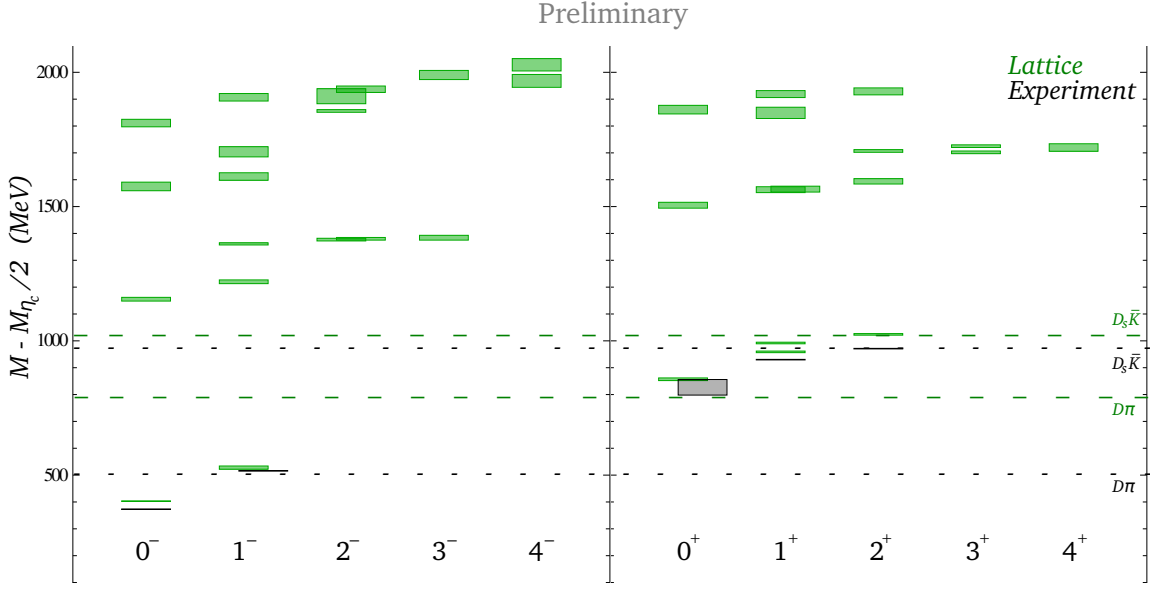


Figure 1: The charm-light (D) meson spectrum up to around 3.8 GeV labelled by J^P . The green boxes are our calculated masses while the black boxes correspond to experimental masses of neutral charm-light mesons from the PDG summary tables [15]. We present the calculated (experimental) masses with half the calculated (experimental) η_c mass subtracted. The vertical size of each box indicates the one sigma statistical uncertainty. The dashed lines show the lowest non-interacting $D\pi$ and $D_s\bar{K}$ thresholds, using our measured masses (coarse green dashed) and experimental masses (fine black dashed).

3.1 Interpretation of results and comparison with experiment

The overlap factors, Z , can aid in the interpretation of extracted states as they can be used to identify their structure. As can be seen in Figs. 1 and 2, the extracted spectrum of states in the charm-light and charm-strange sectors follow a similar pattern. Most of the states fit into the $n^{2S+1}L_J$ pattern expected by quark potential models, where n is the radial quantum number, S is the spin of the quark-antiquark pair, L is the relative orbital angular momentum and J is the total spin of the meson.

In the negative parity sector of both spectra we find an S -wave pair $[0^-, 1^-]$ along with their first and second excitations ~ 700 MeV and ~ 1400 MeV respectively higher. Also in the negative parity sector, we find a full D -wave set $[(1, 2, 3)^-, 2^-]$ at ~ 1400 MeV, what appears to be parts of an excited D -wave set and parts of a G -wave set $[(3, 4, 5)^-, 4^-]$ at ~ 2000 MeV. We do not observe the 5^- state needed to complete the G -wave set but this is to be expected; we only use operators subduced from those that have continuum spins $0 \leq J \leq 4$. Operators that contain four derivatives will possess the required angular structure to access states of spin five.

In the positive parity sector we calculate a full P -wave set $[(0, 1, 2)^+, 1^+]$ around the $D_s\bar{K}$ threshold in the charm-light spectrum and around the DK threshold in the charm-strange spectrum. About 600 MeV higher in both spectra we find the first excitations of the P -wave set. We also see a full F -wave set $[(2, 3, 4)^+, 3^+]$ at ~ 1700 MeV in both spectra.

In the negative parity sector of both spectra we observe four states at ~ 1600 MeV that appear to be supernumerary to the pattern of states predicted by quark potential models. Due to their

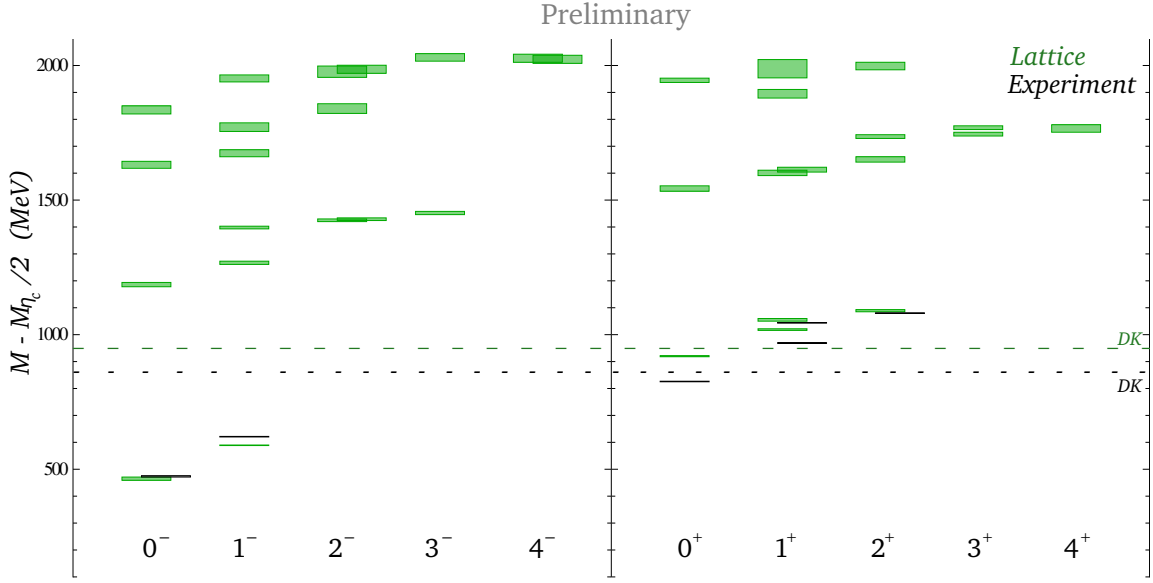


Figure 2: As Fig. 1 but for the charm-strange (D_s) meson spectrum. The dashed lines indicate the lowest non-interacting DK threshold using our measured masses (coarse green dashing) and using experimental masses (fine black dashing).

strong overlap with operators proportional to the field strength tensor we interpret these states as the lightest supermultiplet of hybrid mesons and highlight them in red in Fig. 3. The pattern of states observed in the supermultiplet is the one expected if a quark-antiquark pair in an S -wave configuration is coupled to a 1^{+-} quasi-gluon, and its appearance at an energy scale ~ 1200 MeV above the lightest quark-antiquark state is in agreement with what was observed in both the light meson sector [16] and the charmonium sector [5].

The four supernumerary states in the positive parity sector ~ 1500 MeV above the lightest conventional quark-antiquark state are also interpreted as candidate hybrid mesons, again due to their relatively strong overlap with operators proportional to the field strength tensor. We note, that in the previous studies of Refs. [5, 16], a first excited supermultiplet of hybrid mesons is observed at a similar energy scale, but we do not complete the supermultiplet as other states in this energy region were not robustly determined.

The pattern of our extracted states agree qualitatively with current experimental determinations but some of our states differ quantitatively. The S -wave hyperfine splittings we calculate differ by ~ 20 MeV from experimental values but this can be explained as an $O(a)$ discretisation effect as in Ref. [5]. In the charm-light sector we find our P -wave states heavier than their experimental counterparts which could be due to our unphysically heavy light quarks (our strange quarks are of the correct scale) and/or interaction with the nearby thresholds. In the charm-strange case, two of our P -wave states are consistent with experiment but the other two states, which are expected to correspond to the enigmatic $D_{s0}^*(2317)^\pm$ and $D_{s1}(2460)^\pm$, are significantly higher than their experimental counterparts. We note that the 0^+ and 1^+ states are very close to, respectively, the DK and D^*K thresholds, and both the experimental and calculated 0^+ states lie the same distance from their appropriate thresholds. This may suggest that the unphysically heavy light quarks are

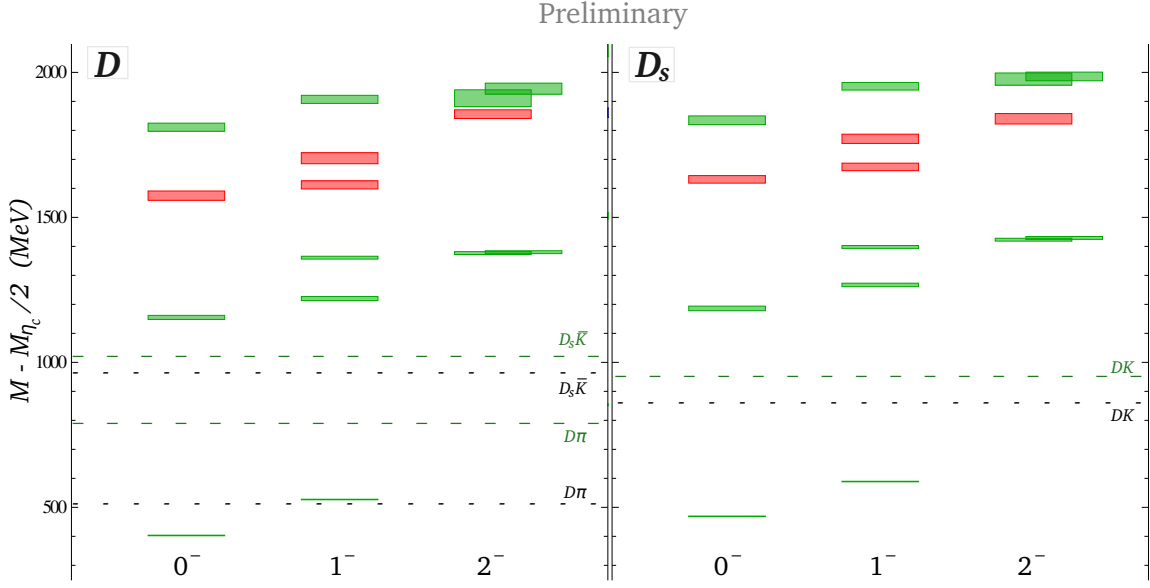


Figure 3: The negative-parity charm-light (left panel) and charm-strange (right panel) meson spectra showing only channels where we identify hybrid candidates. The red boxes are identified as states belonging to the lightest hybrid supermultiplet as discussed in the text and other notation is as in Figs. 1 and 2.

a major contribution to the discrepancy. However, because of the interaction with the threshold, further study is required with multi-hadron operators included in our bases.

4. Summary and outlook

We have presented preliminary spectra in both the charm-light and charm-strange sectors on $N_f = 2 + 1$ dynamical ensembles generated by the Hadron Spectrum Collaboration. The use of a large basis of carefully constructed operators along with a variational analysis has allowed us to extract a large number of states. Our spin identification scheme is crucial to our interpretation as it allows us to identify the J^P of not only the low-lying states but also the highly excited states.

We have identified candidate hybrid mesons due to their relatively strong overlap with operators proportional to the field strength tensor. We observe a pattern of states that is consistent with the lightest hybrid supermultiplet found in previous studies of the light meson [16] and charmonium sectors [5].

In the near future we plan to further study the open-charm sector via calculations along the lines of Refs. [17, 18].

Acknowledgements

We thank our colleagues within the Hadron Spectrum Collaboration. Chroma [19] and QUDA[20, 21] were used to perform this work on the Lonsdale cluster maintained by the Trinity Centre for High Performance Computing funded through grants from Science Foundation Ireland (SFI), at

the SFI/HEA Irish Centre for High-End Computing (ICHEC), and at Jefferson Laboratory under the USQCD Initiative and the LQCD ARRA project. Gauge configurations were generated using resources awarded from the U.S. Department of Energy INCITE program at the Oak Ridge Leadership Computing Facility at Oak Ridge National Laboratory, the NSF Teragrid at the Texas Advanced Computer Center and the Pittsburgh Supercomputer Center, as well as at Jefferson Lab. This research was supported by Science Foundation Ireland under Grant Nos. RFP-PHY-3201 and RFP-PHY-3218. GM acknowledges support from the School of Mathematics at Trinity College Dublin. CET acknowledges support from a Marie Curie International Incoming Fellowship, PIFI-GA 2010-273320, within the 7th European Community Framework Programme.

References

- [1] BABAR Collaboration, J. Aubert *et al.*, Phys. Rev. Lett. 90 (2003) 242001, [arXiv:0304021].
- [2] CLEO Collaboration, D. Besson *et al.*, Phys. Rev. D68 (2003) 032002, [arXiv:0305100].
- [3] S. Godfrey and N. Isgur, Phys. Rev. D32 (1985) 189.
- [4] F. Close and E Swanson, Phys. Rev. D72 (2005) 094004, [arXiv:0505206].
- [5] Hadron Spectrum Collaboration, L. Liu *et al.*, JHEP 07 (2012) 126, [arXiv:1204.5425].
- [6] L. Liu *et al.*, AIP Conf. Proc. 1441 (2012) 324-328.
- [7] R. G. Edwards, B. Joo and H.-W. Lin, Phys. Rev. D78 (2008) 054501, [arXiv:0803.3960].
- [8] H.-W. Lin *et al.*, Phys. Rev. D79 (2009) 034502, [arXiv:0810.3588]
- [9] Hadron Spectrum Collaboration, M. Peardon *et al.*, Phys Rev D80 (2009) 054506, [arXiv:0905.2160].
- [10] J. J. Dudek *et al.*, Phys. Rev. D82 (2010) 034508, [arXiv:1004.4930].
- [11] M. Lüscher and U. Wolff, Nucl. Phys. B339 (1990) 222-252.
- [12] C. Michael, Nucl. Phys. B 259 (1985) 58.
- [13] J. J. Dudek *et al.*, Phys. Rev. Lett. 103 (2009) 262001, [arXiv:0909.0200].
- [14] Z. Davoudi and M. J. Savage, Phys. Rev. D86 (2012) 054505, [arXiv:1204.4146].
- [15] Particle Data Group Collaboration, J. Beringer *et al.*, Phys. Rev. D86 (2012) 010001.
- [16] J. J. Dudek, Phys. Rev. D84 (2011) 074023, [arXiv:1106.5515].
- [17] J. J. Dudek, R. G. Edwards, and C. E. Thomas, Phys. Rev. D86 (2012) 034031, [arXiv:1203.6041].
- [18] J. J. Dudek, R. G. Edwards, C. E. Thomas, [arXiv:1212.0830]
- [19] SciDAC Collaboration, R.G. Edwards and B. Joo, Nucl. Phys. B. Proc. Suppl. 140 (2005) 832, [arXiv:0409003].
- [20] M. A. Clark *et al.*, Comput. Phys. Commun. 181 (2010) 1517-1528, [arXiv:0911.3191].
- [21] R. Babich, M. A. Clark and B. Joo, in International Conference for High Performance Computing, Networking, Storage and Analysis (SC), pp. 1-11, 2010, [arXiv:1011.0024].